

Nuclear structure properties with an updated Gogny force

Goriely S.*

*Institut d'Astronomie et d'Astrophysique, Université Libre de Bruxelles,
Campus de la Plaine CP 226, B-1050 Brussels, Belgium*

Hilaire S. and Girod M.

CEA, DAM, DIF, F-91297, Arpajon, France

(Dated: February 11, 2009)

The increasing need for nuclear data far from the valley of stability requires information on nuclei which cannot be accessed experimentally or for which almost no experimental data is known. Consequently, the use of microscopic approaches to predict properties of such poorly known nuclei is necessary as a first step to improve the quality of nuclear data evaluations. Within this context, large scale mean field calculations from proton to neutron drip-lines have been performed using the Hartree-Fock-Bogoliubov method based on the D1S Gogny nucleon-nucleon effective interaction. Thousands of nuclei have been studied under the axial symmetry hypothesis and several properties are now available for the nuclear scientific community on an Internet web site for every individual nucleus. However, this extensive study has evidenced a severe deficiency of the D1S interaction with respect to the description of the nuclear masses. The present work consists in showing how updated interactions can solve the D1S deficiency while keeping its good properties. In particular, it is shown that the latest interaction is also well suited for an accurate determination of nuclear masses. The first mass table based on Gogny HFB calculations including an explicit and coherent account of all the quadrupole correlation energies is presented.

I. INTRODUCTION

Thanks to the experimental progress achieved in the last decade (as well as to future facilities), more and more nuclei or nuclear states of unusual structure (exotic nuclei, large deformations, isomers, high spins, etc ...) have been (or are going to be) produced. The study of their properties represents a very promising research domain for nuclear physics as well as a challenging test for nuclear structure theories which have mainly been designed to describe stable nuclei or at least located not too far from the valley of stability. An accurate description of more exotic nuclei properties implies that nuclear structure theories must be able to treat correctly the isospin degree of freedom. Such a quest for a theory having a good predictive power has been a very active field of modern nuclear structure theory [1–6] for the last ten years to test and improve the quality of the nuclear structure predictions, and eventually provide the nuclear physics community with systematic predictions based on sound physical bases rather than on extrapolations of phenomenological approaches [6–8].

In ref. [5], large scale Hartree-Fock-Bogoliubov (HFB) axial mean field calculations based on the D1S [9] Gogny interaction have shown that the D1S interaction does not provide good agreement between theoretical and experimental masses. In particular, a systematic drift has been observed for the differences between experimental and theoretical binding energies for almost all isotopic chains. In fact, the D1S Gogny force underbinds the heavier iso-

topes as compared to the lighter ones, and this deficiency remains even when beyond mean field dynamical effects are accounted for [10]. On the contrary this interaction displays a rather good predictive power when looking at different nuclear structure properties such as those of the lowest 2^+ levels [11], the giant resonances [12], the backbending of moments of inertia [13–15], the charge and transition charge densities [16], the shape coexistences [17, 18] or shape isomers [19, 20], the superdeformed bands [21], as well as fission fragment properties [22].

Our goal in this work is thus to determine a new Gogny force parameterization which enables to describe simultaneously nuclear structure properties and masses. In other words, we want to improve the nuclear binding energies predictions without degrading the aforementioned good properties already obtained with the D1S interaction.

II. THE STARTING POINT

A first step towards our goal has been performed introducing the D1N interaction [23]. The main improvement compared to D1S was to improve the fit of the neutron matter which turned out to be the main reason for the drift of the binding energy differences $\delta B = B_{\text{exp}} - B_{\text{th}}$ (as function of the neutron number for an isotopic chain) obtained with the D1S parameterization. The resulting δB values, as illustrated in Fig. 1(a), do not display any systematical drift but still show an oscillating structure with minima located around magic neutron numbers. Because the HFB method is based on an Harmonic Oscillator (HO) basis involving a finite number N of major shells, it is well established that absolute en-

*Electronic address: sgoriely@astro.ulb.ac.be

ergy predictions are sensitive to the adopted number of shell N . Therefore, as in [10], it is necessary to estimate

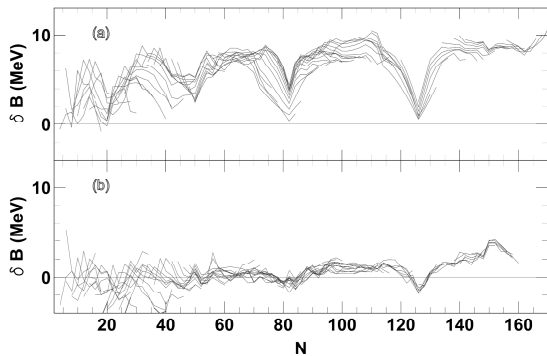


FIG. 1: Difference δB between the theoretical and experimental [24] nuclear binding energies as functions of the neutron number N for different isotopic chains using the D1N interaction. Upper panel : Axially symmetric HFB calculations with finite Harmonic Oscillator bases D1N. Lower panel : Full calculations including infinite basis and quadrupole energy corrections as detailed in the text.

what would be the obtained binding energies $B_{th}(\infty)$ if HFB calculations were performed with an infinite number of shells. To estimate this value, we use the procedure described in [10, 25] to deduce what we call the infinite basis correction $\delta E_{\infty}(N)$ corresponding to the difference between the binding energy $B_{th}(N)$ of a nucleus obtained using N major shells and $B_{th}(\infty)$. On top of these infinite basis corrections, we also have to account for beyond-mean-field quadrupole correlations obtained by solving the collective Schrödinger equation with the 5-dimensional Bohr Hamiltonian [11, 21]. As expected [2], it can be observed in Fig. 1(b) that including these quadrupole energy corrections δE_{quad} washes out the arches of Fig. 1(a). Quantitatively speaking, the overall root mean square (rms) deviation obtained once all the required corrections are included is of the order of 1.5 MeV which is certainly not comparable to the level of accuracy reached by the most sophisticated mass formulae reaching values of the order of 600 to 800 keV [26–30]. Nevertheless, the D1N parameterization is already a step towards our final goal. Indeed, the systematic drift of the binding energies has been suppressed, and, on top of that, the good properties of D1S remain approximately unchanged. For instance, we compare in Fig. 2 the pairing properties of D1S and D1N for the Sn isotopes using the odd-even mass difference $\Delta^{(3)}B = B(A) - \frac{1}{2}[B(A+1) + B(A-1)]$ for odd- A values, which provides a good measure of the amount of pairing along isotopic chains [31]. As can be observed, both parameterizations provide almost equivalent values. Similar conclusions can be drawn when looking at other properties [23]. A nice illustration is given the properties of lowest 2^+ levels. Using the same beyond-mean-field methods that have been used in [11], we show in Fig. 3 a

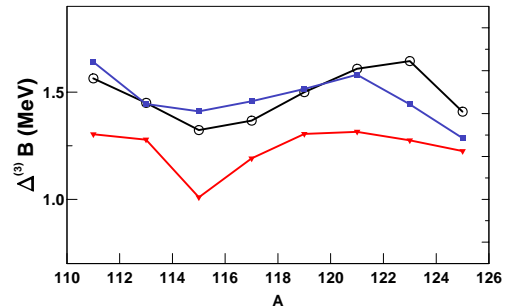


FIG. 2: $\Delta^{(3)}B$ as a function of the nucleon number A in Sn isotopes. Experimental data correspond to the full triangles, D1S to the empty circles and D1N to the full squares.

scatter plot comparing experimental and theoretical excitation energies both for D1S and D1N. In both panels, the points follow the diagonal line fairly well showing that there is no deficiency of the D1N interaction compared to what was obtained with D1S. Performing similar analysis as in [11] by examining the statistical properties of the quantity $R_E = \log(E_{th}/E_{exp})$, we obtain an average value $\bar{R}_E = 0.12$ with D1S which is slightly better than $\bar{R}_E = 0.19$ obtained using D1N and a dispersion which confirms what appears rather well on the scatter plot, i.e. the D1S values ($\sigma_R = 0.33$) are significantly less scattered than the D1N values ($\sigma_R = 1.10$).

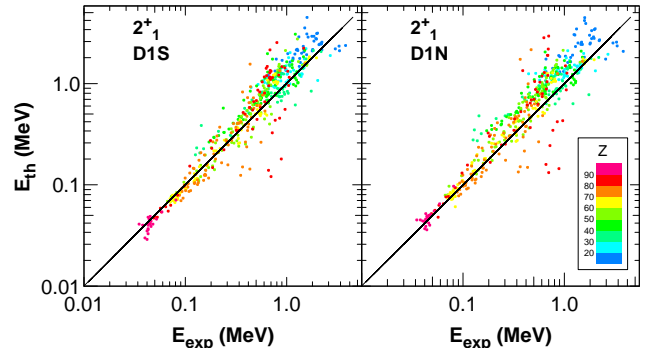


FIG. 3: Scatter plot of the experimental versus theoretical 2^+ excitation energies for the 519 even-even nuclei for which experimental data is available.

III. THE METHODOLOGY TO IMPROVE THE MASS PREDICTIONS

While the D1N force is found suitable to estimate most of the nuclear structure properties, the accuracy of its mass predictions remains unsatisfactory with respect with modern mass formulae reaching a rms devia-

tion of about 0.7 MeV on all the 2149 measured masses [24]. For this reason, a new Gogny force has been obtained by fitting its parameters to virtually all nuclear mass data, keeping as additional constraint the need to provide a satisfactory description of all the nuclear properties mentioned in Sect. II.

In the previous section, we have seen two correction terms had to be determined to produce a theoretical nuclear binding energy that can be compared with experimental masses. If the binding energy $B_{\text{th}}(N)$ obtained using N major shells can be determined within a reasonable computation time, this is not the case for both $\delta E_{\infty}(N)$ and δE_{quad} . Therefore, in order to avoid untractable calculations, the adjustment of the Gogny force parameters to reproduce at best the experimental masses, is not performed by systematically calculating these correction terms. Instead, the computational scheme illustrated by Fig. 4 is followed. The construc-

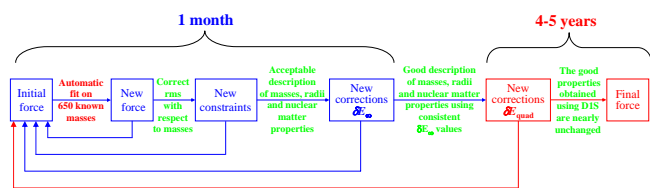


FIG. 4: Computational scheme followed to adjust the Gogny force parameters on nuclear masses, radii as well as selected nuclear matter properties. Among the 14 parameters of the Gogny force, 2 are kept unchanged and 12 parameters are adjusted during the first two steps of the procedure. Iterations back to the initial step occur when the green criteria are not fulfilled. The indicated computation times are given for a single CPU.

tion of the new interaction follows several steps. The first step consists in determining some of the Gogny force parameters reproducing at best selected nuclear matter properties known to play a key role with respect to the good properties of the D1S/D1N Gogny force. The remaining parameters are then automatically fitted on a subset of 650 measured nuclear masses. To determine the rms with this reduced set, it is necessary to include the two corrections $\delta E_{\infty}(N)$ and δE_{quad} . To avoid performing the aforementioned time consuming calculation of these corrections, we assume that $\delta E_{\infty}(N)$ and δE_{quad} are not modified during the first three steps of our procedure and we accordingly take for these correction terms the values that have been tabulated with a previous force. At the beginning of our fit, these corrections correspond to the values obtained with D1N. When we consider the rms obtained using this set of 650 masses to be acceptable, we then extend our calculation to the 2149 measured masses compiled in [24] (Note that we also consider the quality of the force with respect to the rms deviation on the measured radii as well as nuclear matter properties). If these new constraints are fulfilled, the δE_{∞} , and then δE_{quad}

corrections are re-estimated with the new force to obtain one unique coherent calculation of the nuclear masses. This procedure is re-iterated until the rms deviation on nuclear masses and radii as well as nuclear matter properties are found satisfactory.

IV. RESULTS

Using the previously described methodology, we have obtained a new Gogny force, called D1M. This force predicts nuclear masses with an rms deviation of 0.798 MeV with respects to all the 2149 measured masses. The rms and mean deviations are summarized in Table I. The mass comparison is shown in Fig. 5. As can be seen, no deviation exceeds 3.2 MeV. The accuracy reached with D1M is comparable to the best available nuclear mass formulas and by far better than the one obtained with the D1N or D1S forces. It should be noted that in the present calculation, no Wigner correction has been included. If we only consider the 2000 nuclei away from the $|N - Z| \leq 2$ line, the rms deviation amounts to 0.771 MeV. However, like in all Skyrme-HFB mass formulas, the theoretical masses in the $N \simeq 126$ region remain significantly overbound. The low effective mass ($m^*/m = 0.75$) or the missing particle-vibration coupling effects can be held responsible for this trend.

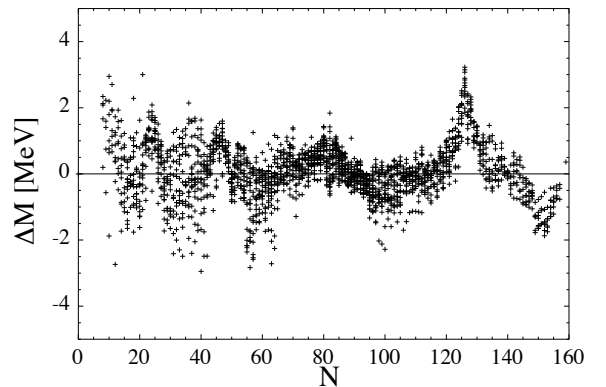


FIG. 5: Differences between measured [24] and theoretical masses as a function of N .

In Fig. 6, we show the neutron matter equation of state obtained with our new D1M parameterization. As can be observed, the results are in close agreement, both with the D1N predictions and the realistic calculation of Friedman-Phandharipande (FP) [33] considered here as the reference curve. Such an agreement is an important constraint since, as explained in Ref. [23], the approximate description of the neutron matter equation of state by the D1S Gogny force was the main reason for the systematic drift observed for the differences between experimental and theoretical binding energies for almost all isotopic chains with D1S Gogny force.

TABLE I: Rms (σ) and mean ($\bar{\epsilon}$) deviations between data [24] and our predictions. The first line refers to all the 2149 measured masses M , the second to the 2000 masses for nuclei with $|N - Z| > 2$, the third to the 1988 measured neutron separation energies S_n and the fourth to 1868 measured beta-decay energies Q_β . The fifth line finally shows the comparison with the 707 measured charge radii [32]

| | σ | $\bar{\epsilon}$ |
|--------------------------|----------|------------------|
| 2149 M [MeV] | 0.798 | 0.126 |
| 2000 $M_{ N-Z >2}$ [MeV] | 0.771 | 0.155 |
| 1988 S_n [MeV] | 0.538 | 0.004 |
| 1868 Q_β [MeV] | 0.657 | 0.015 |
| 707 R_{ch} [fm] | 0.031 | -0.008 |

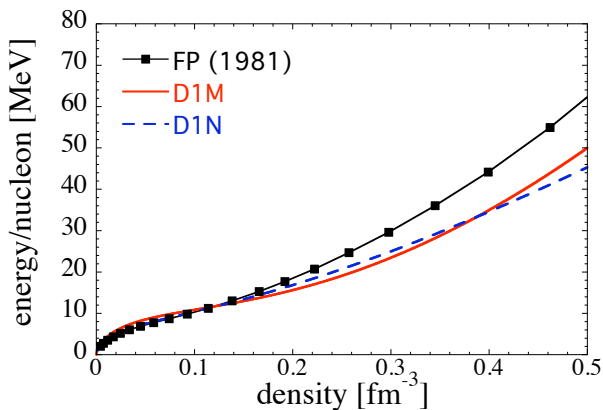


FIG. 6: Energy per neutron (MeV) as a function of density (fm^{-3}) of neutron matter for D1N (dashed line), the New interaction (solid line) and for the calculations of Ref. [33] (FP; symbols)

Figure 7 compares the D1M potential energy per particle for symmetric nuclear matter in each of the four two-body spin-isospin (S, T) channels with the Brueckner-Hartree-Fock calculation obtained with realistic two- and three-nucleon forces [34]. A fair agreement between our new force and the realistic calculations can be seen in all states, except in the even-singlet channel which is constrained by the pairing. In this respect, the pairing properties of our new interaction are relatively similar to those of D1S and D1N. In contrast to D1N predictions, we obtain the correct sign for the isovector splitting of the effective mass, i.e a higher neutron than proton effective mass $m_n^* > m_p^*$ at all asymmetries. Such an isovector splitting of the effective mass is consistent with measurements of isovector giant resonances [35], and has been confirmed in several many-body calculations with realistic forces [36].

Our new D1M force has also been tested with respect to various additional observables, such as the kinetic moment of inertia in Er or Pu nuclei, the giant monopole, dipole and quadrupole energy in ^{208}Pb derived within

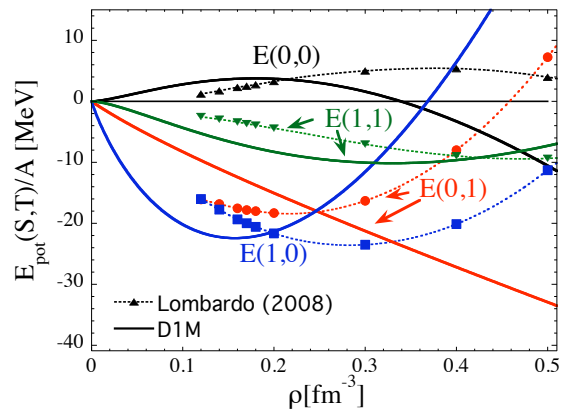


FIG. 7: Potential energy per particle in each (S, T) channel as a function of the density for symmetric infinite nuclear matter. The full symbols (connected with the dashed lines) correspond to Brueckner-Hartree-Fock calculations [34] and the solid lines to D1M.

the random-phase approximation, and the energy of the lowest 2^+ levels for the 519 even-even nuclei for which experimental data is available. For all these observables, the new force gives results very similar to those obtained

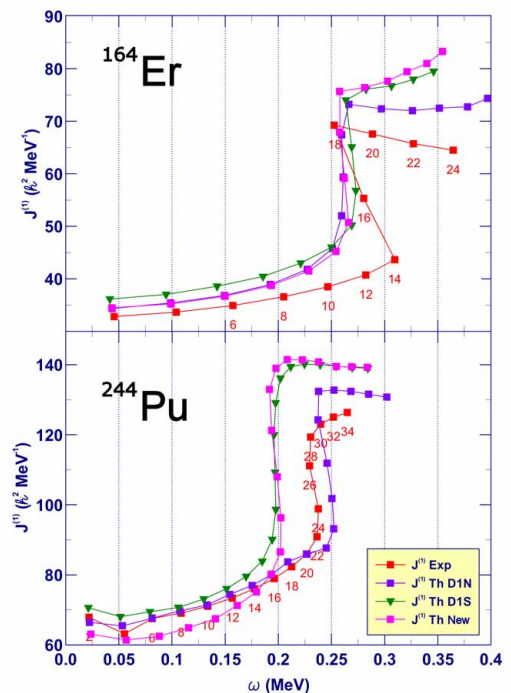


FIG. 8: Comparisons between experimental kinetic moments of inertia with the cranking HFB predictions based on D1S, D1N and D1M forces for ^{164}Er (upper panel) and ^{244}Pu (lower panel). The moments of inertia are plotted as a function of the rotational frequency.

with D1S. An illustration is given in Fig. 8 where the

^{164}Er and ^{244}Pu kinetic moment of inertias, known to be rather well reproduced in superfluid nuclei [37], are plotted using the D1S, D1N and D1M parameterizations. As can be seen, the experimentally observed backbending occurs with the three parameterizations. For ^{244}Pu , the D1N interaction gives predictions in closer agreement with experimental data.

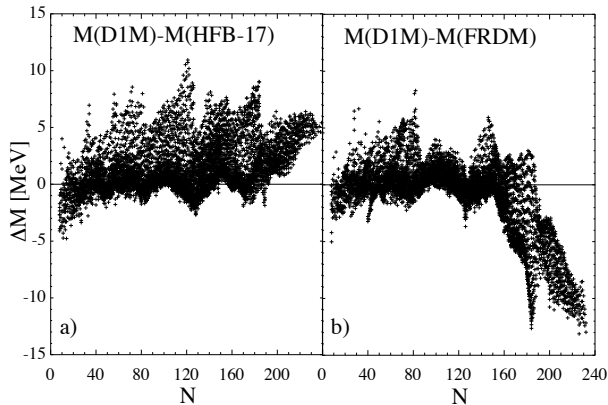


FIG. 9: Differences between a) Our New force and HFB-17 masses [38] and b) Our New force and FRDM masses [39].

On the basis of the new D1M force, we have constructed a complete mass table going from one drip line to the other over the range Z and $N \geq 8$ and $Z \leq 110$.

In Fig.9, we compare these predictions with those of the "best-fit" Skyrme-HFB model (HFB-17) [38] and with those of the FRDM [39]. In both cases we see that despite the close similarity in the quality of the fits to the data, large differences emerge, especially for heavy nuclei when the neutron-drip line is approached. The triaxially deformed calculation also enable us to estimate the energy correction related to the nuclear triaxial deformation. The $Z \simeq 62$ and $N \simeq 74$ region is found to be the most deformed one with a triaxial correction energy reaching about 0.4 MeV.

V. CONCLUSIONS

We have described the first Gogny-HFB nuclear mass model. The rms deviation with respect to essentially all the available mass data has been reduced from typically a few MeV with previous interactions to less than 0.8 MeV. Furthermore, for the first time, the mass formula takes an explicit and self-consistent account of all the quadrupole correlations affecting the binding energy. The quadrupole corrections are estimated microscopically on the basis of a 5-dimensional Bohr Hamiltonian. Given also the constraint imposed on the Gogny force by microscopic calculations of neutron matter and symmetric nuclear matter, this new model is particularly well adapted to astrophysical applications such as the r-process of nucleosynthesis.

-
- [1] E. Chabanat et al., Nucl. Phys. A **627** (1997) 710; **635** (1998) 231; **643** (1998) (E) 441.
 - [2] M. Bender, G.F. Bertsch and P.-H. Heenen, Phys. Rev. Lett. **94** (2005) 102503; Phys. Rev. C **73** (2006) 034322.
 - [3] M.V. Stoitsov, J. Dobaczewski, W. Nazarewicz, S. Pittel and D.J. Dean, Phys. Rev. C **68** (2003) 054312.
 - [4] B. Sabbey, M. Bender, G.F. Bertsch and P.-H. Heenen, Phys. Rev. C **75** (2007) 044305.
 - [5] S. Hilaire and M. Girod, Eur. Phys. J. A **33** (2007) 237.
 - [6] S. Goriely and J.M. Pearson, Phys. Rev. C **77** (2008) 031301 and references therein.
 - [7] S. Goriely and E. Khan, Nucl. Phys. A **706** (2002) 217.
 - [8] S. Hilaire and S. Goriely, Nucl. Phys. A **779** (2006) 63.
 - [9] J.F. Berger, M. Girod and D. Gogny, Comp. Phys. Comm. **63** (1991) 365.
 - [10] S. Hilaire and M. Girod, in Proceedings of the International Conference on Nuclear Data for Science and Technology, April 22-27 2007, Nice, France, editors O. Bersillon et al., EDP Sciences (2008) p. 107-110.
 - [11] G. F. Bertsch et al., Phys. Rev. Lett. **99** (2007) 032502.
 - [12] S. Péru, J. F. Berger and P. F. Bortignon, Eur. Phys. J. A **26** (2005) 25.
 - [13] J.P. Delaroche, M. Girod, H. Goutte and J. Libert, Nuc. Phys. A **771** (2006) 103.
 - [14] J.L. Egido and L.M. Robledo, Nuc. Phys. A **570** (1994) 69.
 - [15] J.L. Egido and L.M. Robledo, Phys. Rev. Lett. **70** (1993) 2876.
 - [16] X.H. Phan et al., Phys. Rev. C **38** (1988) 1173; **39** (1989) (E) 1645.
 - [17] J. Ljungvall et al., Phys. Rev. Lett. **100** (2008) 102502.
 - [18] E. Clement et al., Phys. Rev. C **75** (2008) 054313.
 - [19] M. Girod, J.P. Delaroche and J.F. Berger, Phys. Rev. C **38** (1988) 1519.
 - [20] M. Girod et al., Phys. Rev. Lett. **62** (1989) 21.
 - [21] J. Libert, M. Girod and J.P. Delaroche, Phys. Rev. C **60** (1999) 054301.
 - [22] N. Dubray, H. Goutte and J.P. Delaroche, Phys. Rev. C **77** (2008) 014310.
 - [23] F. Chappert, M. Girod and S. Hilaire, Phys. Lett. B **668** (2008) 420.
 - [24] G. Audi, A.H. Wapstra and C. Thibault, Nucl. Phys. A **729** (2003) 337.
 - [25] J. Dechargé and L. Sips, Nucl. Phys. A **407** (1983) 1.
 - [26] P. Möller, J.R. Nix, W.D. Myers and W.J. Swiatecki, At. Data. Nucl. Data Tables **59** (1995) 185.
 - [27] S. Goriely, M. Samyn, P.-H. Heenen, J.M. Pearson and F. Tondeur, Phys. Rev. C **66**, (2002) 024326.
 - [28] S. Goriely, M. Samyn, M. Bender and J.M. Pearson, Phys. Rev. C **68** (2003) 054325.
 - [29] H. Koura, M. Uno, T. Tachibana and M. Yamada, Nucl. Phys. A **674** (2000) 47.

- [30] J. Duflo and A.P. Zuker, Phys. Rev. C **52** (1995) R23.
- [31] W. Satula, J. Dobaczewski, and W. Nazarewicz, Phys. Rev. Lett. **81** (1998) 3599.
- [32] I. Angeli, At. Data and Nucl. Data Tables **87**, 185 (2004).
- [33] B. Friedman and V. R. Pandharipande, Nucl. Phys. **A361**, 502 (1981).
- [34] U.Lombardo, Private communication (2008); see also Z.H. Li, U. Lombardo, H.J. Schulze, and W. Zuo, Phys. Rev. **C77**, 034316 (2008).
- [35] T. Lesinski, K. Bennaceur, T. Duguet, and J. Meyer, Phys. Rev. C **74**, 044315 (2006).
- [36] W. Zuo, U. Lombardo, H.-J. Schulze, and Z. H. Li, Phys. Rev. C **74**, 014317 (2006).
- [37] J.L. Egido and L.M. Robledo, Phys. Rev. Lett. **70** (1993) 2876.
- [38] S. Goriely, N. Chamel and J. M. Pearson, submitted to PRL (2009).
- [39] P. Möller and J. R. Nix, At. Data Nucl. Data Tables **39**, 213, (1988).